

Simulation Of A Three Level Boosting PFC With Sensorless Capacitor Voltage Balancing Control

1. S.DIVYA, PG Student, 2. C. Balachandra Reddy, Professor & HOD
Department of EEE, CBTVIT, Hyderabad

Abstract - Compared with the conventional boosting PFC converter, the three-level boosting PFC converter has two cascaded switches and two cascaded capacitors across the dc-side voltage. Two capacitor voltages may be different due to their mismatched equivalent series resistance, their mismatched capacitance, and the mismatched conducting time of the corresponding switches. It follows that the controller needs to sense the capacitor voltages to balance both capacitor voltages. In this paper, the sensorless capacitor voltage balancing control (SCVBC) without sensing the capacitor voltages is proposed, and the total number of the feedback signals is saved. The proposed SCVBC is digitally implemented in an FPGA-based system. The provided simulated and experimental results also demonstrate the proposed SCVBC.

I. Introduction

To reduce the power transmission loss and increase the system stability, more and more power-electronics products are forced to include the power factor correction (PFC) function. Generally speaking, the PFC function includes shaping the ac-side current waveform and regulating the dc-side voltage. Due to the characteristics of the continuous current, the boost-derived PFC converters have been widely used to achieve the desired PFC function. For the conventional boost dc/dc converter, the single switch needs to withstand the dc output voltage when the single switch blocks. Two cascaded switches and two cascaded capacitors are connected together in the three-level boosting dc/dc converter. When one of the switches conducts and the other blocks, the blocking switch needs to withstand only half dc output voltage if both capacitor voltages are balanced. If not balanced, one of the capacitor voltages may be larger than the breakdown voltage of the switch, which would contribute to make damage to the switch. It is noted that the inductor voltage in the three-level boost dc/dc converter has three levels, which makes the three-level boosting dc/dc converter to have smaller inductor current ripple

often used in the high-voltage-ratio applications, such as the fuel cell applications and the grid-connected applications. In addition, the high-withstanding-voltage semiconductor switches often have higher cost and the larger drain-source resistances than the low-withstanding-voltage ones. Thus, the three-level boost converter has the additional advantages of the low switching loss and the high efficiency. The three-level boosting PFC converter was first proposed in by connecting the diode rectifier to the three-level boosting dc/dc converter. In the multiloop interleaved control combining the multiloop control and the interleaved PWM scheme was first proposed to control the three-level boosting PFC converter. the multiloop control includes the feed forward loop, the inner current loop, and the outer voltage loop. The three single-phase three-level boosting PFC converter in Delta connection is used to achieve the three-phase PFC function with the ability of redundancy. However, the balance between two capacitor voltages should be noted. In practice, the mismatched capacitances and the mismatched equivalent series resistance (ESR) would result in the voltage imbalance. Therefore, the control of the three-level boosting converter needs to balance both capacitor voltages. In the literature, the voltage balancing control loop for three-level boosting converters can be found. In fact, the other voltage balancing control can be found in the controls of the half-bridge PFC converter and the multilevel inverter. All the methods need to sense capacitor voltages to detect the voltage imbalance and yield the desired voltage balancing function. The multiloop interleaved control with conventional capacitor voltage balancing control (CVBC). One control signal is generated by the multiloop control, and the other control signal is yielded by CVBC with sensing the capacitor voltages. For the three-level boosting dc/dc converter, a voltage balancing control method with sensing only inductor current was first proposed in. In this paper, the concept in is extended to the three-level boosting PFC application and the proposed controller is named the sensorless capacitor voltage balancing control (SCVBC). The voltage imbalance between two capacitor voltages is skillfully detected by sensing the inductor current. The detailed analysis and the design rule of the proportion-type voltage balance controller are also provided. It follows that sensing individual capacitor voltage is not

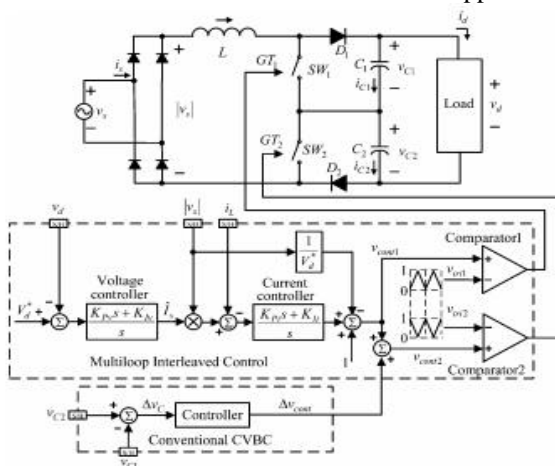


Fig. 1. Three-level boosting PFC converter with multiloop feedforward control and the conventional capacitor voltage balancing control loop
than the boost converter under the same switching frequency. Therefore, the three-level boost converters are

required, and at least one voltage sensor is saved. The provided simulation and experimental results show the effectiveness of the proposed SCVBC.

II. LITERATURE SURVEY

The input ac voltage $v_s = \hat{V} \sin(2\pi ft)$ is assumed to be a sinusoidal function with a peak amplitude \hat{V} . Through the diode rectifier, the input voltage of the three-level boosting converter can be expressed with the rectified voltage $|v_s|$. By assuming that the switching frequency f_s is much larger than the line frequency f , the control signals v_{cont1} and v_{cont2} can be regarded as two constants within the switching period $T_s = 1/f_s$. In addition, the ideal inductor and the ideal capacitors are assumed. That is, the inductor resistance and the capacitor resistances are assumed to be zero. In Fig. 1, two triangular signals v_{tri1} and v_{tri2} are interleaved by 180° . The conventional multiloop control generates the control signal v_{cont1} , and then, the gate signal GT1 is generated from the comparison of the control signal v_{cont1} and the triangular signal v_{tri1} . After sensing both capacitor voltages, the voltage imbalance is detected and the conventional CVBC generates the compensation signal v_{cont} . Then, the other control signal v_{cont2} is obtained by adding the compensation signal v_{cont} to the control signal v_{cont1} . The gate signal GT2 is obtained from the comparison of the control signal v_{cont2} and the triangular signals v_{tri2} . Due to the input inductor L and two diodes D1 and D2 in the three-level boosting PFC converter, both switches can be conducting at the same time without the concern of the shortcircuit damage. As plotted in Fig. 2, there are four switching states in the three-level boosting PFC converter. As shown in Fig. 2(a), both switches turn ON in the switching state 1. Thus, the inductor voltage v_L in the three-level.

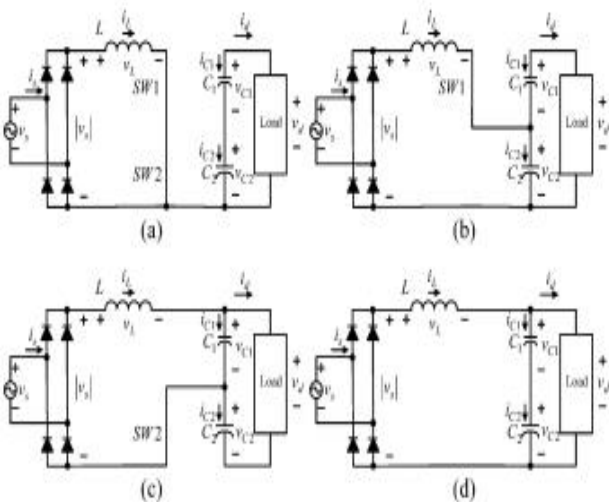


Fig. 2. Possible switching states in the three-level boosting PFC converter: (a) state 1, (b) state 2, (c) state 3, and (d) state 4

Table I capacitor currents in each state

		state 1	state 2	state 3	state 4
$2 > v_{cont1} + v_{cont2} > 1$	i_{C1}	$-i_d$ (<0)	$-i_d$ (<0)	$i_L - i_d$ (>0)	
	i_{C2}		$-i_d$ (<0)	$i_L - i_d$ (>0)	$-i_d$ (<0)
$1 > v_{cont1} + v_{cont2} > 0$	i_{C1}		$-i_d$ (<0)	$i_L - i_d$ (>0)	$i_L - i_d$ (>0)
	i_{C2}		$i_L - i_d$ (>0)	$-i_d$ (<0)	$i_L - i_d$ (>0)

boosting PFC converter equals the rectified input voltage $v_L = |v_s|$ and both capacitors supply energy to the load $i_{C1} = i_{C2} = (-i_d) < 0$. In the switching state 2 in Fig. 2(b), the top switch turns ON and the bottom switch turns OFF. The resulting inductor voltage v_L equals the rectified input voltage $|v_s|$ minus the bottom capacitor voltage $v_L = |v_s| - v_{C2}$. Additionally, the capacitor C1 supplies energy to the load $i_{C1} = (-i_d) < 0$, but the capacitor C2 stores the energy from the input voltage $i_{C2} = (i_L - i_d) > 0$. Similarly, the resulting inductor voltage in Fig. 2(c) equals the rectified input voltage minus the top capacitor voltage $v_L = |v_s| - v_{C1}$. In the switching state 3, the top capacitor C1 is charged $i_{C1} = (i_L - i_d) > 0$, but the bottom capacitor C2 is discharged $i_{C2} = (-i_d) < 0$. When both switches turn OFF in Fig. 2(d), the resulting inductor voltage equals the rectified input voltage minus the output voltage $v_L = |v_s| - v_d = |v_s| - v_{C1} - v_{C2}$. The rectified input voltage $|v_s|$ supplies the load current and charges both capacitors simultaneously $i_{C1} = i_{C2} = (i_L - i_d) > 0$. All the capacitor currents in various switching states are tabulated in Table I. The behavior of the three-level boosting converter can be divided into two cases as shown in Fig. 3. In the case of $2 > v_{cont1} + v_{cont2} > 1$, two switches may conduct at the same time within the switching period T_s and there are switching state 1, state 2, and state 3. In the other case of $1 > v_{cont1} + v_{cont2} > 0$, only switching state 2, state 3, and state 4 exist.

III. PROPOSED METHOD AND RESULTS

The multiloop interleaved control and the proposed SCVBC with the proposed sampling/hold strategy are where only the input voltage v_s , the output voltage v_d , and the inductor current i_L are sensed. It is noted that the proposed sampling/hold strategy samples the inductor current i_L thrice per switching period T_s , and obtains the average value I_L and the other two values I_{vC1} and I_{vC2} . The average value current I_L is input to the multiloop control to yield the desired PFC function and obtain the control signal v_{cont1} . The difference $I_{vC2} - I_{vC1}$ between two values I_{vC1} and I_{vC2} is calculated and the compensating signal v_{cont} is obtained by the used P controller

$$\Delta v_{cont} = K_p(I_{vC2} - I_{vC1}) \tag{6}$$

Then, the other control signal v_{cont2} is generated by adding the compensating signal v_{cont} to the control signal v_{cont1}

$$v_{cont2} = v_{cont1} + \Delta v_{cont} = v_{cont1} + K_p(I_{vC2} - I_{vC1}). \quad (7)$$

the proposed sampling/hold strategy with sensing the inductor current i_L . The average value I_L is obtained by sampling the inductor current i_L at the peak of the triangular signal $v_{tri1} = 1$. When the triangular signal v_{tri1} rises to 0.5 from the valley, the inductor current is sampled and the obtained

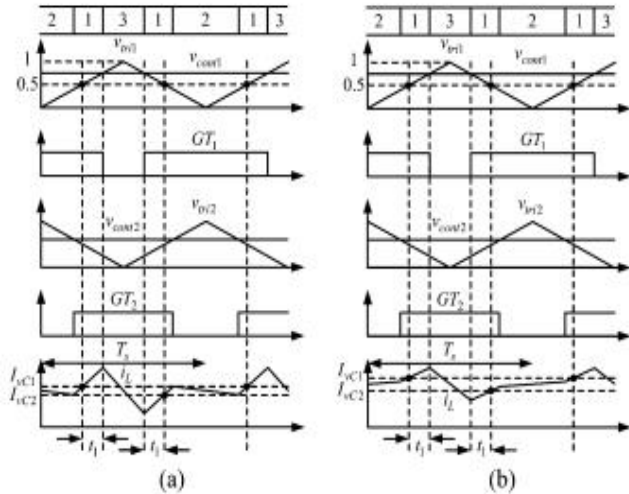


Fig. 7. Illustrated waveforms($2 > v_{cont1} + v_{cont2} > 1$). (a) $v_{C1} > v_{C2} > |v_s|$ and (b) $v_{C1} > |v_s| > v_{C2}$. value is defined as I_{vC1} . The value I_{vC2} is sampled when the triangular signal v_{tri1} falls to 0.5 from the peak. After finishing all the sampling actions, the multiloop control is performed at the controller time, and updates the two control signals at the valley of the triangular signal v_{tri1} . In the following paragraphs, the analysis is divided into two cases - $2 > v_{cont1} + v_{cont2} > 1$ and $1 > v_{cont1} + v_{cont2} > 0$

$$2 > v_{cont1} + v_{cont2} > 1.$$

The illustrated waveforms for the voltage imbalance $v_C > 0$ (i.e., $v_{C1} > v_{C2}$) are plotted in. Since the input ac voltage v_s is time-varying, the voltage imbalance $v_C > 0$ may be divided into two conditions—either $v_{C1} > v_{C2} > |v_s|$ or $v_{C1} > |v_s| > v_{C2}$. The waveforms in the condition $v_{C1} > v_{C2} > |v_s|$ are plotted in, and the inductor current i_L is falling at the switching state 2. But the inductor current i_L is rising at the switching state 2 in the other condition $v_{C1} > |v_s| > v_{C2}$ as plotted in. The illustrated waveforms for the voltage imbalance $v_C < 0$ ($v_{C2} > v_{C1} > |v_s|$ and $v_{C2} > |v_s| > v_{C1}$) are plotted in respectively. It is noted that in, the inductor current i_L is falling at the switching state 3, but the current i_L is rising at the switching state 3 in. Due to the waveform symmetry in, the time t_1 between the instants of sampling the value I_{vC1} and the turning-off instants of the gate signal $GT1$ is equal to the time between the turning-on instants of the gate signal $GT1$ and the instants of sampling the value I_{vC2} . Therefore, the time t_1 can be expressed in terms of the control signal v_{cont1}

$$t_1 = \left(\frac{v_{cont1}}{2} - \frac{1}{4} \right) T_s. \quad (8)$$

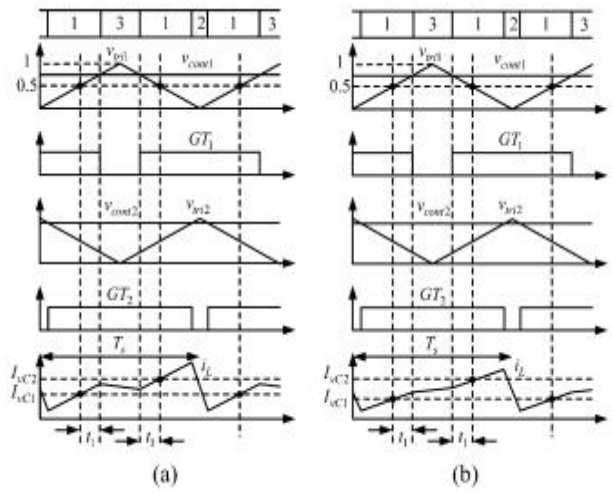


Fig. 8. Illustrated waveforms($2 > v_{cont1} + v_{cont2} > 1$). (a) $v_{C2} > v_{C1} > |v_s|$ and (b) $v_{C2} > |v_s| > v_{C1}$. the conducting time for the switching state 2 and the switching state 3 are $(1 - v_{cont2})T_s$ and $(1 - v_{cont1})T_s$, respectively. The remaining time for switching state 1 is $(v_{cont1} + v_{cont2} - 1)T_s$. Then, the average inductor voltage $v_L T_s$ in the three-level boosting converter can be expressed as equation (9) at the bottom of the page. Because of zero average inductor voltage in the steady-state condition, the rectified input voltage $|v_s|$ must be equal to

$$|v_s| = (1 - v_{cont1})v_{C1} + (1 - v_{cont2})v_{C2}. \quad (10)$$

the difference I_{vC} between two sampled values I_{vC1} and I_{vC2} can be expressed in terms of the time t_1

$$\Delta I_{vC} = I_{vC2} - I_{vC1} = 2 \frac{|v_s|}{L} t_1 + \frac{|v_s| - v_{C1}}{L} (1 - v_{cont1}) T_s. \quad (11)$$

Substituting (8) and (10) into (11) obtains

$$\Delta I_{vC} = \frac{T_s}{2L} [(v_{C2} - v_{C1})(1 - v_{cont1}) - \Delta v_{cont} v_{C2}]. \quad (12)$$

By substituting (6) into (12), the expression I_{vC} in (12) can be rewritten as

$$\Delta I_{vC} = \frac{I_s(1 - v_{cont1})}{2L + T_s K_P v_{C2}} (v_{C2} - v_{C1}) = k_1 (v_{C2} - v_{C1}). \quad (13)$$

Because the coefficient k_1 is always positive, the difference I_{vC} is proportional to the voltage imbalance $(v_{C2} - v_{C1})$. It follows that the difference I_{vC} can be used to detect the voltage imbalance $(v_{C2} - v_{C1})$ without directly sensing the capacitor voltages. $1 > v_{cont1} + v_{cont2} > 0$

$$\langle v_L \rangle_{T_s} = \frac{|v_s|(v_{cont1} + v_{cont2} - 1)T_s + (|v_s| - v_{C1})(1 - v_{cont1})T_s + (|v_s| - v_{C2})(1 - v_{cont2})T_s}{T_s} \tag{9}$$

$$= |v_s| - v_{C1}(1 - v_{cont1}) - v_{C2}(1 - v_{cont2})$$

illustrated waveforms for the voltage imbalance $v_{C1} > v_{C2} > |v_s|$ and $v_{C1} > v_{C2} > |v_s|$ are plotted respectively. In the inductor current i_L is rising at the switching state 3, but the inductor current i_L is falling at the switching state 3. The illustrated waveforms for the voltage imbalance $|v_s| > v_{C2} > v_{C1}$ and $v_{C2} > |v_s| > v_{C1}$ are plotted respectively. It is noted that in the inductor current i_L is rising at the switching state 2 due to $|v_s| > v_{C2}$, but the current i_L is falling at the switching state 2 in due to $v_{C2} > |v_s|$. Due to the symmetry, the time t_2 between the instants of sampling the value I_{vC1} and the turning-off instants of the gate signal GT_1 can be expressed in terms of the control signal v_{cont1}

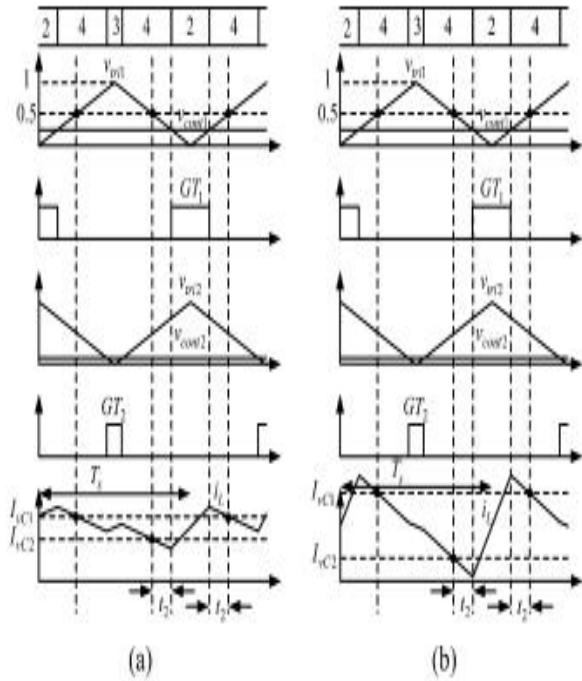


Fig. 9. Illustrated waveforms ($1 > v_{cont1} + v_{cont2} > 0$). (a) $|v_s| > v_{C1} > v_{C2}$ and (b) $v_{C1} > |v_s| > v_{C2}$.

$$t_2 = \left(\frac{1}{4} - \frac{v_{cont1}}{2} \right) T_s \tag{14}$$

the conducting times for switching state 2 and switching state 3 are $(v_{cont1}T_s)$ and $(v_{cont2}T_s)$, respectively. The remaining times in a switching period T_s for switching state 4 is $(1 - v_{cont1} - v_{cont2})T_s$. The average inductor voltage $v_L T_s$ in the three-level converters is the same as (9), equation (15), the difference I_{vC} between two sampled values I_{vC1} and I_{vC2} can be expressed in terms of the time

$$\Delta I_{vC} = I_{vC2} - I_{vC1} = -\frac{|v_s| - v_{C2}}{L} v_{cont1} T_s - 2 \frac{|v_s| - v_d}{L} t_2 \tag{16}$$

Substituting (10) and (14) into (16) obtains

$$\Delta I_{vC} = \frac{T_s}{2L} [(v_{C2} - v_{C1})v_{cont1} + \Delta v_{cont} v_{C2}] \tag{17}$$

By substituting (6) into (17), (17) can be rewritten as

$$\Delta I_{vC} = \frac{T_s v_{cont1}}{2L - T_s K_P v_{C2}} (v_{C2} - v_{C1}) = k_2 (v_{C2} - v_{C1}) \tag{18}$$

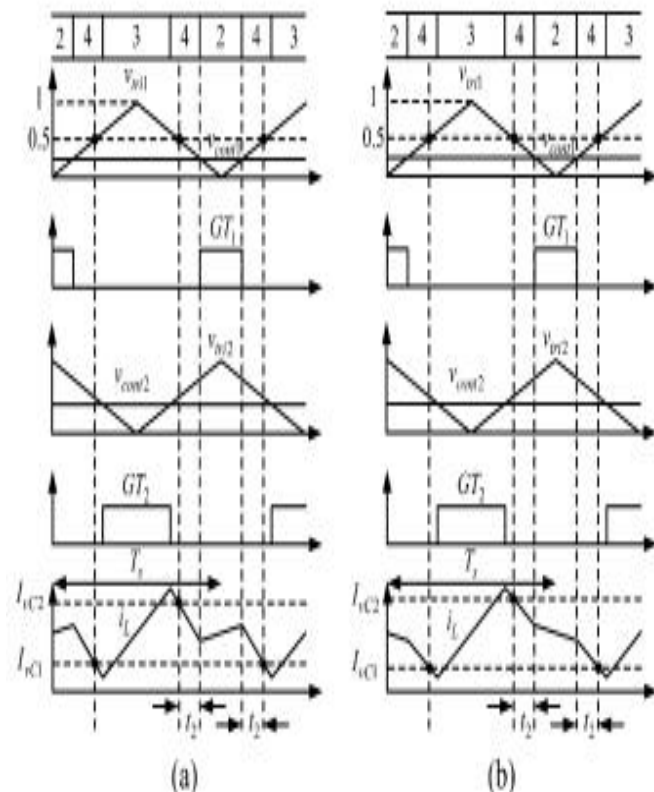
The coefficient k_2 may be either positive one or negative one. In order to force the coefficient k_2 positive, the denominator should be positive

$$2L - T_s K_P v_{C2} > 0 \tag{19}$$

It implies that the controller parameter K_P should be located at the range

$$0 < K_P < \frac{2L}{T_s v_{C2, \max}} \tag{20}$$

Where $v_{C2, \max}$ is the maximum bottom capacitor voltage. Then, the difference I_{vC} would be proportional to the voltage imbalance $(v_{C2} - v_{C1})$. From (13) and (18) in both cases, the difference I_{vC} in both cases are proportional to the voltage imbalance $(v_{C2} - v_{C1})$ via properly selecting the controller parameter K_P , which implies that the difference I_{vC} obtained from the proposed SCVBC can be used to detect the voltage imbalance $(v_{C2} - v_{C1})$ without directly sensing the capacitor voltages.



Illustrated waveforms ($1 > v_{cont1} + v_{cont2} > 0$). (a) $|v_s| > v_{C2} > v_{C1}$ and (b) $v_{C2} > |v_s| > v_{C1}$. In this case, the

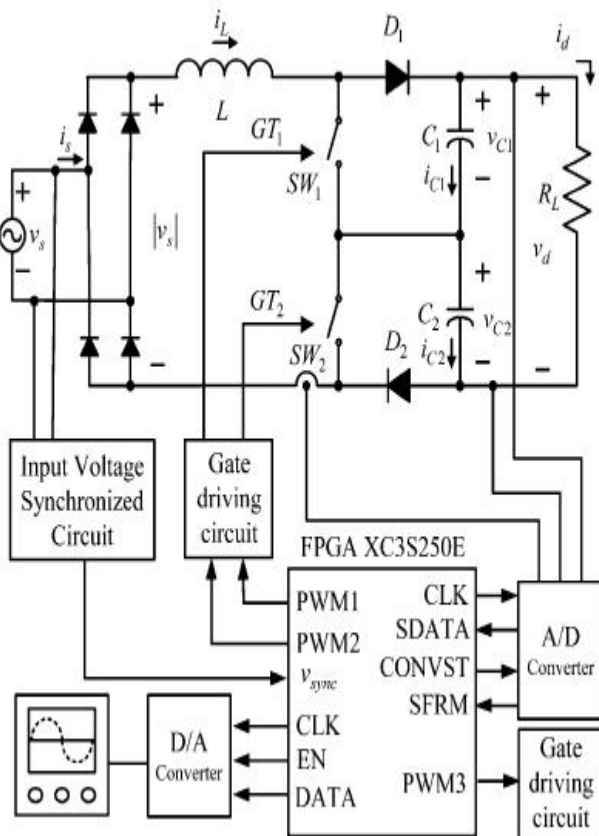


Fig. 16. Block diagram of the implemented three-level boosting PFC converter

CONCLUSION

In this paper, the SCVBC method for the three-level boosting PFC converter has been proposed. The proposed method shows that the voltage imbalance can be detected from sensing the inductor current by the proposed sampling/hold strategy. That is, it eliminates the need for extra sensors, reduces control complexity, and reduces the cost and size. The reduction of cost and size are the important contributions for PFC converters. The control method is implemented in an FPGA-based system, and all the provided results demonstrate the proposed method.

REFERENCES

- [1] B. Singh, B. N. Singh, A. Chandra, K. Al-Haddad, A. Pandey, and D. P. Kothari, "A review of single-phase improved power quality ACDC converters," *IEEE Trans. Ind. Electron.*, vol. 50, no. 5, pp. 962–981, Oct. 2003.
- [2] J. C. Crebier, B. Revol, and J. P. Ferrieux, "Boost-chopper-derived PFC rectifiers: Interest and reality," *IEEE Trans. Ind. Electron.*, vol. 52, no. 1, pp. 36–45, Feb. 2005.
- [3] L. S. Yang, T. J. Liang, H. C. Lee, and J. F. Chen, "Novel high step-up DC–DC converter with coupled-inductor and voltage-doubler circuits," *IEEE Trans. Ind. Electron.*, vol. 58, no. 9, pp. 4196–4206, Sep. 2011.
- [4] A. Shahin, M. Hinaje, J. P. Martin, S. Pierfederici, S. Rael, and B. Davat, "High voltage ratio DC–DC converter for fuel-cell applications," *IEEE Trans. Ind. Electron.*, vol. 57, no. 12, pp. 3944–3955, Dec. 2010.
- [5] M. H. Todorovic, L. Palma, and P. N. Enjeti, "Design of a wide input range DC–DC converter with a robust power control

scheme suitable for fuel cell power conversion," *IEEE Trans. Ind. Electron.*, vol. 55, no. 3, pp. 1247–1255, Mar. 2008.

[6] W. Li and X. He, "Review of nonisolated high-step-Up DC/DC converters in photovoltaic grid-connected applications," *IEEE Trans. Ind. Electron.*, vol. 58, no. 4, pp. 1239–1250, Apr. 2011.

[7] J. M. Kwon, B. H. Kwon, and K. H. Nam, "Three-phase photovoltaic system with three-level boosting MPPT control," *IEEE Trans. Power Electron.*, vol. 23, no. 5, pp. 2319–2327, Sep. 2008.

[8] V. Yaramasu and B. Wu, "Three-level boost converter based medium voltage megawatt PMSG wind energy conversion systems," in *Proc. Energy Convers. Cong. Expo.*, 2011, pp. 561–567.

[9] M. T. Zhang, Y. Jiang, F. C. Lee, and M. M. Jovanovic, "Single-phase three-level boost power factor correction converter," in *IEEE App. Power Electron. Conf.*, 1995, pp. 434–439.

[10] J. R. Pinheiro, D. L. R. Vidor, and H. A. Grunding, "Dual output threelevel boost power factor correction converter with unbalanced loads," in *Proc. IEEE Power Electron. Spec. Conf.*, 1996, pp. 733–739.

[11] B. R. Lin and H. H. Lu, "A novel PWM scheme for single-phase threelevel power-factor-correction circuit," *IEEE Trans. Ind. Electron.*, vol. 47, no. 2, pp. 245–252, Apr. 2000.

[12] H. Wu and X. He, "Single phase three-level power factor correction circuit with passive lossless snubber," *IEEE Trans. Power Electron.*, vol. 17, no. 6, pp. 946–953, Nov. 2002.

[13] J. Y. Liao and H. C. Chen, "Multiloop interleaved control for two-switch two-capacitor three-level SMR without capacitor voltage balancing loop," in *Proc. IEEE Energy Convers. Congr. Expo.*, 2011, pp. 3766–3772.

[14] R. Greul, S. D. Round, and J. W. Kolar, "The Delta-Rectifier: Analysis, Control and Operation," *IEEE Trans. Power Electron.*, vol. 21, no. 6, pp. 1637–1648, Nov. 2006.

[15] E. Ribeiro, A. J. M. Cardoso, and C. Boccaletti, "Fault-tolerant strategy for a photovoltaic DC–DC converter," *IEEE Trans. Power Electron.*, vol. 28, no. 6, pp. 3008–3018, Jun. 2013.

[16] R. Ghosh and G. Narayanan, "A simple analog controller for single phase half-bridge rectifier," *IEEE Trans. Power Electron.*, vol. 22, no. 1, pp. 186–198, Jan. 2007.

[17] B. R. Lin, T. L. Huang, and C. H. Huang, "Bi-directional single-phase half-bridge rectifier for power quality compensation," *IEE, Electric Power Appl.*, vol. 150, no. 4, pp. 397–406, July 2003.

[18] Z. Shu, N. Ding, J. Chen, H. Zhu, and X. He, "Multilevel SVPWM with DC-link capacitor voltage balancing control for diode-clamped multilevel converter based STATCOM," *IEEE Trans. Ind. Electron.*, vol. 60, no. 5, pp. 1884–1896, May 2013.

[19] C. Gao, X. Jiang, Y. Li, Z. Chen, and J. Liu, "A DC-link voltage selfbalancing method for a diode-clamped modular multilevel converter with minimum number of voltage sensors," *IEEE Trans. Power Electron.*, vol. 28, no. 5, pp. 2125–2139, May 2013.